

Heterogeneous photo-Fenton degradation of phenolic aqueous solutions over iron-containing SBA-15 catalyst

F. Martínez, G. Calleja, J.A. Melero* and R. Molina

Department of Chemical, Environmental and Materials Technology. ESCET.
Rey Juan Carlos University. C/ Tulipán s/n, 28933. Móstoles, Madrid (Spain).

Published on:

Applied Catalysis B: Environmental 60 (2005) 181–190

[doi:10.1016/j.apcatb.2005.03.004](https://doi.org/10.1016/j.apcatb.2005.03.004)

Keywords: Photo-Fenton, heterogeneous catalysts, SBA-15, experimental design and phenol

* Corresponding author: Phone: 34 91 4887087. Fax: 34 91 4887068 E-mail: j.melero@escet.urjc.es (J.A. Melero)

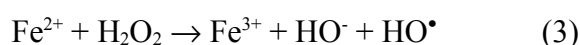
ABSTRACT

A novel iron-containing mesostructured material has been successfully tested for the heterogeneous photo-Fenton degradation of phenolic aqueous solutions using near UV-visible irradiation (higher than 313 nm) at room temperature and close to neutral pH. This catalyst is a composite material that contains crystalline hematite particles embedded into the mesostructured SBA-15 matrix in a wide distribution of size (30 – 300 nm) and well dispersed ionic iron species within the siliceous framework. The outstanding physico-chemical properties make this material a promising photocatalyst leading to better activity than other unsupported iron oxides. An experimental design model has been applied to assign the weight of catalyst and hydrogen peroxide concentrations in the photo-Fenton processes over this particular material. The catalytic performance has been monitored in terms of aromatics and total organic carbon (TOC) conversions, whereas the catalyst stability was evaluated according to the metal leached into the aqueous solution. Hydrogen peroxide concentration plays an important role in the stability of the iron species, preventing their leaching out into the solution, in contrast to the effect shown in typical dark Fenton reaction. The homogeneous leached iron species result in very little contribution to the overall photocatalysis process. Catalyst loadings of 0.5 g/L and concentration of hydrogen peroxide close to the stoichiometric amount have yielded a total abatement of phenol and a remarkable organic mineralization.

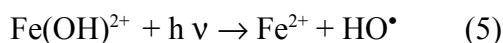
1. Introduction

During the last decade the abatement of aromatic compounds in wastewaters has been an important challenge due to their bio-toxicity and refractory behavior for the microorganisms as well as their hazard carcinogenic effects for human being. The application of Advanced Oxidation Technologies (AOT's) like the one presented in this study have emerged as an important alternative for the efficient removal of organic pollutants, being nowadays widely described in the literature [1-2]. These novel destruction techniques are based on the generation of hydroxyl radicals which are able to mineralize refractory chemicals present in effluent water.

The oxidation system based on the Fenton's reagent (hydrogen peroxide in the presence of ferric ions) has been used as a powerful source of oxidative radicals [3]:



More recently, Fenton processes has been shown to be enhanced by light due to the decomposition of the photoactive $\text{Fe}(\text{OH})^{2+}$ species, promoting an additional generation of OH^\bullet radicals in solution [4]:



However, it has been reported that Fenton homogeneously catalyzed reactions needs concentrations of ca. 50-80 ppm of iron ions in solution which is quite above the 2 ppm permitted by the European Community Directives [5]. Therefore, in order to remove the iron ions from solution, precipitation and re-dissolution techniques are necessary with the additional operational costs. This reason has promoted the development of dark- and photo-Fenton processes based on heterogeneous catalytic systems, which provide an easy separation and recovery of the catalyst from the treated wastewater. Unlike homogeneous Fenton reaction, where a strict control of pH around 2-3 is required for a good catalytic performance, immobilized Fenton catalytic systems provide the possibility of working in a wider pH range. The crucial point of heterogeneous catalytic systems is linked to the resistance of immobilized iron species to be leached out into the solution under the typically acidic and strong oxidizing conditions in which Fenton reactions occur. In this way, research efforts are currently addressed to design new photocatalysts with high stability and allowing an efficient use of the hydrogen peroxide due to its relative high cost. Thus, one of the aims in this research field should be to prepare stable materials that require the lowest oxidant to catalyst ratio for obtaining good degradation rates.

In the literature, different organic and inorganic materials have been already reported as supports for the immobilization of active iron species in heterogeneous photo-Fenton processes. Nafion, as films or pellets, has been employed as organic support due to the presence of sulphonic groups allowing the effective anchoring of Fe ions [6-8]. However, Nafion materials show a low photocatalytic activity and are not very attractive due to their relative high cost. More recently, a novel Fe/C structured fabric has been successfully used for the complete discoloration of Orange II, but a high hydrogen peroxide to substrate ratio was needed [9]. Among inorganic supports, some type of zeolites and pillared clays have been

also used. Iron (III) doped-Y zeolitic material, prepared by ion exchange techniques, was used for degradation of poly(vinyl alcohol) [10]. However, a low catalytic activity was achieved in terms of the remaining levels of dissolved organic carbon after 2 hours of treatment. These Fe exchanged zeolites have been also tested in the photo-assisted degradation of phenol with a low initial phenol concentration of 100 ppm and a stoichiometric amount of hydrogen peroxide [11]. Nanosized Fe_2O_3 particle oxides intercalated as pillars between layered clays such as laponite and bentonite have revealed a high photocatalytic activity for discoloration and mineralization of different dyes, but using high energetic 254 nm UV irradiation [12-14].

The purpose of this study is the assessment of a novel composite Fe-containing SBA-15 mesostructured material for the heterogeneous photo-Fenton degradation of phenolic aqueous solutions. Power irradiation light and hydrogen peroxide consumption are the main parameters to be considered in photo-Fenton processes due to their economical importance. High energetic 254 nm UV radiation used by some authors [12-15] has been substituted by UV near visible irradiation (> 313 nm) in this contribution, which represents a significant advantage for future application in solar photodegradation processes. Additionally, hydrogen peroxide to iron ratio has been proven to play an important role in homogeneous photo-Fenton processes [16] but few details are reported for heterogeneous photo-Fenton systems. In the present work, multivariate analysis has been used to assess the conditions (oxidant and catalyst concentrations) that yield the best result in terms of organic degradation and catalyst stability.

2. EXPERIMENTAL

2.1. Preparation of catalyst

Iron-containing SBA-15 mesostructured material has been prepared by co-condensation of iron ($\text{FeCl}_3 \cdot 6\text{H}_2\text{O}$; Aldrich) and silica (tetraethoxysilicate, TEOS; Aldrich) sources under acidic conditions and templated with Pluronic 123 as described elsewhere [17]. The precipitation of crystalline iron oxide particles was promoted by ageing of the resultant solution at 110 °C for 24 hours under static conditions and pH of 3.5. After ageing step, the solid product was recovered by filtration and air dried at room temperature overnight. The template was removed by calcination in air at 550°C for 5 hours.

Commercial hematite with a BET surface area of 60 m²/g was purchased from Aldrich with the purpose of comparison.

2.2. Characterisation

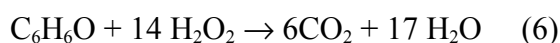
X-ray powder diffraction data were acquired on a PHILIPS X-PERT diffractometer using Cu K α radiation. The data were collected from 2θ ranging from 0.5 to 90° with a resolution of 0.02°. Nitrogen adsorption and desorption isotherms at 77 K were measured using a Micromeritics Tristar 3000 equipment. The data were analysed using the BJH model and the pore volume (V_p) was taken at $P/P_0 = 0.975$ single point. Transmission electron microscopy (TEM) microphotographs and energy dispersive X-ray (EDX) microanalysis were carried out on a PHILIPS TECNAI-20 electron microscope operating at 200 kV. Bulk iron content of the

prepared sample was obtained by Atomic Emission Spectroscopy with Induced Coupled Plasma (ICP-AES) analysis collected in a Varian Vista AX system.

2.3. Photo-Fenton reactions

Photo-Fenton catalytic runs were carried out in a Pyrex batch cylindrical reactor containing 1 L of the aqueous dispersion of the catalyst and the pollutant. The reactor was provided on the top with three ports for inflow and outflow of gases and withdrawal of aliquots for their analysis. The irradiation was performed with a 150W medium pressure mercury lamp (Heraeus TQ-150) inside a quartz jacket, immersed in the mixture and coaxial with the photoreactor. The lamp was surrounded by a cooling tube in which a copper sulphate aqueous solution was circulating to prevent overheating of the suspension and cutting off radiation with a wavelength shorter than 313 nm.

Prior to photo-Fenton experiments, the corresponding amount of catalyst was dispersed in 980 mL of deionised water and introduced in the reactor. Simultaneously, the lamp was immersed in the reactor and switched on during 15 minutes before adding the phenol and hydrogen peroxide reagents, in order to avoid the inherent induction time of the irradiation source. Thereafter, a concentrated phenol solution with the required amount of hydrogen peroxide was added to the reactor up to obtain 1L of aqueous solution. The temperature was maintained at 25 °C during all the reaction time. The initial concentrations were 500 ppm for phenol and 4100 to 800 ppm for hydrogen peroxide. The stoichiometric oxidant concentration required for the total oxidation of phenol is 2550 ppm, according to the following reaction:



Aliquots of 8 ml were taken at selected reaction times and filtered by means of 0.22 μm nylon membranes before being analysed. The phenol conversion was monitored with a HPLC chromatograph Varian Prostar apparatus equipped with a Waters Spherisorb column (250 x 4.6 mm) and an UV detector at 215 nm. The analysis of other by-products coming from the incomplete mineralization of phenol was also performed by this technique. Total organic carbon (TOC) content of the solutions before and after reaction was measured with a combustion/non dispersive infrared gas analyser model TOC-V Shimadzu. Aromatic removal (X_A) in percentage of carbon was calculated as follows:

$$X_A (\%) = \frac{\text{Initial TOC (ppm of C)} - \text{ppm of C from aromatics measured by HPLC}}{\text{Initial TOC (ppm of C)}} \times 100$$

Hydrogen peroxide concentration after reaction was evaluated by iodometric titration. Iron content in the filtered solution after reaction was measured by ICP-AES analysis collected in a Varian VISTA AX system.

3. RESULTS AND DISCUSSION

3.1 Catalyst properties

Iron-containing SBA-15 material was firstly characterized by XRD. Low angle XRD spectrum, depicted in Figure 1, clearly shows (100), (110) and (200) reflections typical of hexagonally mesostructured SBA-15 materials [18]. Additionally, the presence of crystalline iron oxides particles has been detected by high angle XRD analysis (Figure 1.b). These crystalline entities show the typical pattern of crystalline hematite (see Figure 1.b, top right). Figure 1.c illustrates the nitrogen adsorption/desorption isotherm of the calcined material as

well as the pore size distribution in the mesopore range. The adsorption results indicate a type IV isotherm with a H1 hysteresis loop typical of mesoporous materials [19]. The calculated BET area for the calcined material is around 468 m²/g which is slightly lower than that usually found for pure silica SBA-15 materials [18]; this might be attributed to the presence of supported hematite entities. Finally, a narrow pore size distribution (see Figure 1.c, top left) confirms the presence of uniform pores of the same size and the high mesoscopic ordering previously inferred from low angle XRD spectrum.

TEM images also confirm the presence of both hematite entities (a broad distribution particle size among 30-300 nm has been established in a previous study [20]) and well ordered channels with 2D hexagonal symmetry typical of SBA-15 materials. Microanalysis measurements show zones with a high concentration of Fe which are related with the micro-aggregates of hematite and low contents for the mesostructured zone (Figure 1.d). The bulk iron content of the sample measured by ICP-AES was 16 wt. %. Moreover, analysis of local iron environment in this material by means of Mössbauer experiments has also confirmed the presence of hematite particles embedded into the mesostructured matrix and iron present in ionic dispersion in the mesostructured siliceous framework [20].

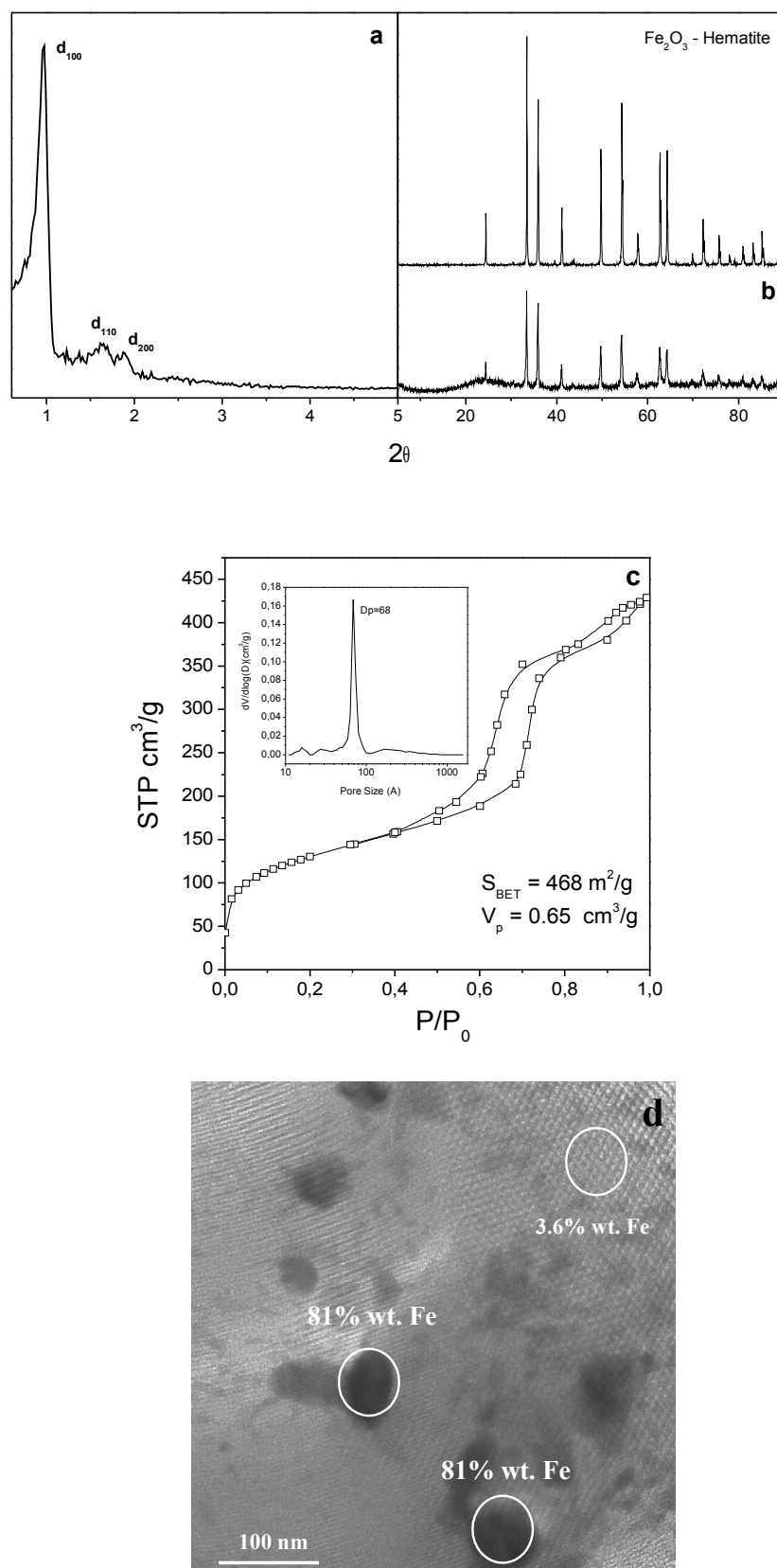
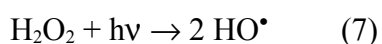


Figure 1. Characterization results of iron-containing SBA-15 material. (a) XRD pattern at low angle range (b) XRD pattern at high angle range (c) nitrogen adsorption/desorption isotherm (pore size distribution in top left) and (d) TEM microphotograph and iron content (% wt.) measured by EDX microanalysis

3.2 Preliminary experiments

The efficiency of iron containing SBA-15 catalyst in the photo-assisted degradation of phenolic aqueous solutions was preliminarily evaluated under different reaction conditions combining the presence of hydrogen peroxide and UV light. Figure 2 shows the evolution of TOC conversion within the reaction time for these experiments. The photo-catalytic activity of Fe-SBA-15 material in presence of a close stoichiometric hydrogen peroxide concentration (2450 ppm; curve 1) shows a significant TOC reduction achieving a conversion value of ca. 50% after 4 hours of reaction. The absence of hydrogen peroxide in analogous reaction conditions (curve 2) leads to just 5% of TOC degradation, which clearly evidences the important role of the hydroxyl radicals coming from photocatalytic decomposition of hydrogen peroxide. Similar TOC reductions are observed in the experiment carried out in absence of UV light and presence of catalyst and hydrogen peroxide (2450 ppm; curve 3). This fact demonstrates the restricted production of hydroxyl radicals by catalytic dark-Fenton reactions at these particular conditions. Note that UV light in absence of catalyst and presence of hydrogen peroxide (2450 ppm; curve 4) yielded a relevant enhancement of TOC conversion, which reveals that hydroxyl radical production by photolytic decomposition of hydrogen peroxide under UV-visible irradiation higher than 313 nm cannot be ruled out (reaction 7).



Finally, the photocatalytic activity of Fe-SBA-15 material has been compared to that obtained with a commercial hematite iron oxide under analogous reaction conditions (curve 5). A low TOC conversion is shown by the commercial iron oxide, which indicates beyond doubt the advantages of supporting small iron oxides particles over the surface of hexagonal

SBA-15 mesostructured materials. However, the role of ionic Fe species in Fe-SBA-15 catalyst could also account for the striking enhancement of TOC removal over this material.

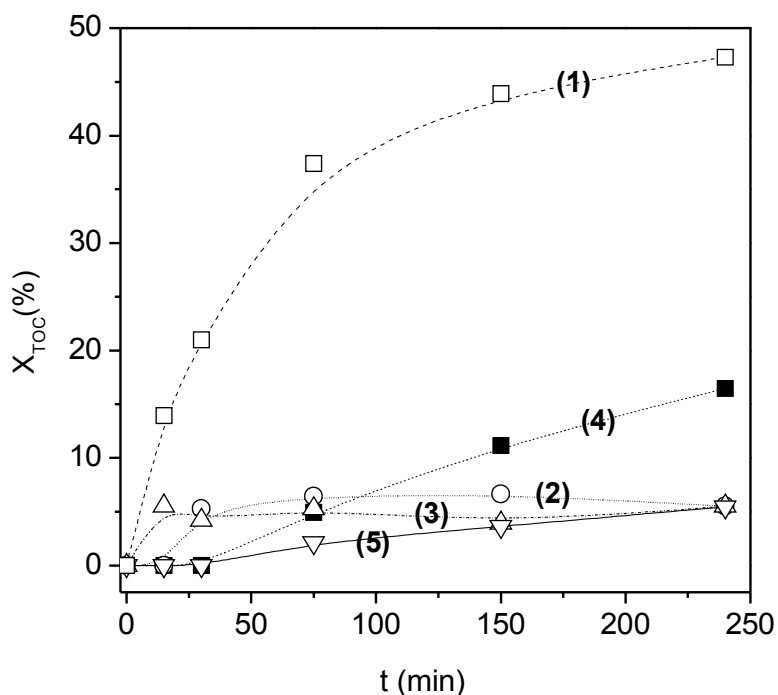


Figure 2. Evolution of TOC conversion along the time under different reaction conditions. $[\text{TOC}]_0=380$ ppm; $[\text{Catalyst}]=0.5$ g/L; Initial pH= 5.5; $T=25$ °C. Photo-catalytic activity of Fe-SBA-15 catalyst in presence (1) and absence (2) of hydrogen peroxide; Dark Fenton reaction over Fe-SBA-15 catalyst (3); Photolysis in presence of hydrogen peroxide (4); Photo-catalytic activity of commercial crystalline hematite in presence of hydrogen peroxide (5).

3.3 Factorial design of experiments for photo-Fenton heterogeneous system

Preliminary experiments have clearly evidenced that immobilized iron species over mesostructured SBA-15 materials present an acceptable catalytic performance for the photo-assisted degradation of phenolic aqueous solutions through Fenton processes. In this second part of the manuscript the influence of significant variables on the reaction has been studied by means of an experimental design methodology. The study was mainly focused on the influence of catalyst and hydrogen peroxide concentrations on the heterogeneous photo-Fenton degradation of phenol over this novel iron-containing material.

A factorial experimental design based on 3^2 [21] was carried out considering low and high levels for Fe-SBA-15 catalyst loadings (0.5-1.5 g/L) and hydrogen peroxide concentration (800-4100 ppm). The choice of this particular range of catalyst concentration was based on the literature data, where similar ranges are generally considered [12, 13, 22]. Optimal concentration of 1 g/L has been in particular reported for photo-Fenton processes catalyzed by iron-containing clays [13]. However, other authors like Cuzzola et al. [23] have also tested higher catalyst loadings, up to 30 g/L, for the treatment of linear alkylbenzene sulphonic acids with Fe(III) supported over γ -Al₂O₃ or SiO₂ under solar irradiation. With respect to the hydrogen peroxide concentration, the range was selected according to other studies described in literature, taking into account that the iron to oxidant ratio is an important variable giving to different mechanisms [24]. Moreover, it should be noted that the oxidant concentration is also strongly dependent on the organic content to be degraded. In this sense, hydrogen peroxide dose has been set in accordance with the initial phenol concentration, being also within the typical iron to oxidant ratio for homogeneous Fenton reactions (1 part of iron per 5-25 parts of hydrogen peroxide (wt./wt.)) [16, 25]. Finally, the efficient use of hydrogen peroxide has also attracted the attention of others in order to minimize the addition of the oxidant [26].

Table 1 describes the factorial design of the experiments, including the codified and real experimental values selected in this work. Low and high levels are denoted by (-1), (+1), respectively, whereas the central point as (0). Central point experiments were repeated three times in order to check the reproducibility and to obtain the standard deviation of the experimental response. The percentage of TOC removal at different reaction times, 30 (Y₁), 75(Y₂), 150(Y₃) and 240 (Y₄) minutes, was chosen as the response factor. The experimental

values of TOC conversion as well as the calculated values obtained from the model are also depicted in Table 1. From the matrix generated by the experimental TOC data and assuming a second order polynomial model, the equations (8), (9), (10) and (11) were obtained for different reaction times using a Levenberg-Marquadt algorithm for nonlinear regression, where X_1 and X_2 represent the catalyst and hydrogen peroxide concentrations, respectively. The magnitude of the interaction between the variables is related with the value of the coefficients of the polynomial expression used to fit the experimental data. Values in parenthesis describe the relative error associated to each coefficient.

Table 1. Numerical data and results of the factorial design of phenol degradation in photo-Fenton reactions

Exp.	Codified values		Y = TOC conversion (%)							
	X_1 [Catalyst]	X_2 [H ₂ O ₂] ₀	Y ₁ (30 min)		Y ₂ (75min)		Y ₃ (150min)		Y ₄ (240 min)	
	g/L	ppm	Exp.	Calc.	Exp.	Calc.	Exp.	Calc.	Exp.	Calc.
1	0.5 (-1)	800 (-1)	23.3	25.7	28.7	31.4	27.4	28.5	29.7	30.0
2	0.5 (-1)	4100 (+1)	34.4	36.8	42.2	44.9	49.7	50.8	59.1	59.4
3	1.5 (+1)	800 (-1)	8.4	10.8	12.1	14.8	23.1	20.1	29.0	23.3
4	1.5 (+1)	4100 (+1)	46.7	49.1	48.9	51.6	55.2	56.3	82.4	82.8
5	1 (0)	2450 (0)	13.1	15.2	16.7	18.4	43.3	42.6	56.1	56.5
6	1 (0)	2450 (0)	12.4	15.2	12.6	18.4	40.3	42.6	55.3	56.5
7	1 (0)	2450 (0)	10.5	15.2	15.3	18.4	39.7	42.6	56.9	56.5
8	0.5 (-1)	2450 (0)	35.9	31.1	39.7	34.3	44.5	42.1	48.1	47.5
9	1.5 (+1)	2450 (0)	40.0	35.2	45.1	39.7	52.6	50.4	61.5	60.9
10	1 (0)	800 (-1)	11.0	6.2	15.7	10.3	35.6	33.4	50.0	49.4
11	1 (0)	4100 (+1)	23.9	19.1	29.3	24.0	39.3	37.1	53.6	53.0

$$Y_1(\% \text{ TOC removal}) = 15.22(\pm 3.6) + 2.04(\pm 4.33) X_1 + 6.42(\pm 3.37) X_2 + 6.78(\pm 2.5) X_1 X_2 + 17.92(\pm 2.5) X_1^2 - 2.56(\pm 1.76) X_2^2 - 2.68(\pm 2.04) X_1 X_2^2 + 5.92(\pm 1.93) X_2 X_1^2 \quad (8)$$

$$Y_2(\% \text{ TOC removal}) = 18.41(\pm 4.1) + 2.72(\pm 4.9) X_1 + 6.79(\pm 4.3) X_2 + 5.81(\pm 2.82) X_1 X_2 + 18.57(\pm 2.8) X_1^2 - 1.31(\pm 2.06) X_2^2 - 5.2(\pm 2.31) X_1 X_2^2 + 5.79(\pm 2.19) X_2 X_1^2 \quad (9)$$

$$Y_3(\% \text{ TOC removal}) = 42.56(\pm 1.8) + 4.16(\pm 2.18) X_1 + 1.84(\pm 2.95) X_2 + 3.46(\pm 1.26) X_1 X_2 + 3.67(\pm 1.27) X_1^2 - 7.31(\pm 0.89) X_2^2 - 4.87(\pm 1.02) X_1 X_2^2 + 12.79(\pm 0.97) X_2 X_1^2 \quad (10)$$

$$Y_4(\% \text{ TOC removal}) = 56.48(\pm 0.57) + 6.7(\pm 0.68) X_1 + 1.8(\pm 0.61) X_2 + 7.51(\pm 0.39) X_1 X_2 - 2.3(\pm 0.4) X_1^2 - 5.3(\pm 0.28) X_2^2 - 2.54(\pm 0.32) X_1 X_2^2 + 20.40(\pm 0.30) X_2 X_1^2 \quad (11)$$

Concerning the equation coefficients shown above, it is clear that quadratic terms are dominant, resulting in a significant curvature of the response surface of TOC removal. The catalyst concentration (X_1^2) is important for initial reaction times, whereas the synergic effect of the catalyst concentration (X_1^2) and the hydrogen peroxide (X_2) becomes dominant for longer reaction times (150 and 240 min) in detrimental to the effect of every individual variable.

3D-Graphical representation of the corresponding equations (8) to (11) are shown in Figures 3. 3D-response surface at 30 minutes (Figure 3.a) clearly shows a decrease of TOC conversion with catalyst loading when the initial hydrogen peroxide concentration is small. This detrimental effect of the catalyst concentration can be attributed to the presence of a significant amount of solid particles, which would reduce the transmission of near UV-visible light and produce scattering of the incident light. A similar effect has been also reported in photocatalytic processes with titanium oxide [1]. However, a significant increase of TOC conversion is obtained using the highest catalyst and oxidant concentrations. Both variables have led to an enhancement of the catalytic performance for heterogeneous like-Fenton reactions in dark conditions [27]. This fact may suggest the presence of a possible coupling of dark-Fenton and photo-Fenton processes as responsible for the overall mineralization of organic matter when high concentrations of oxidant and catalyst are present in the reaction medium. A similar behavior is observed after 75 minutes of reaction (Figure 3.b). For longer reaction times (150 and 240 min; Figures 3.c and 3.d respectively), the increase of catalyst loadings at low hydrogen peroxide concentration exhibits a convex-like 3D surface response curves of TOC conversion, in contrast to the concave shapes shown for lower reaction times.

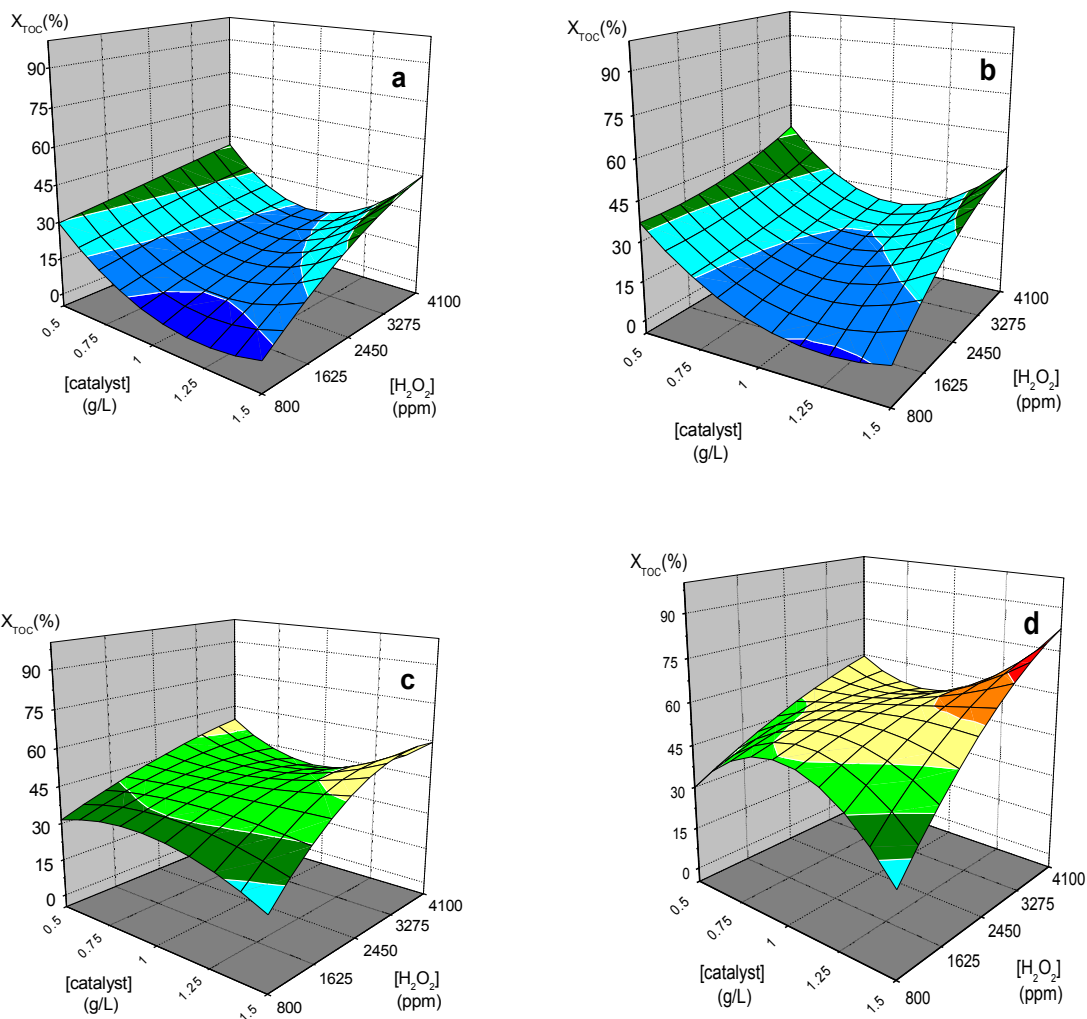


Figure 3. 3D response surfaces of TOC conversion for: a) 30 minutes , b) 75 minutes , c) 150 minutes and d) 240 minutes. $[TOC]_0=380$ ppm; Initial pH= 5.5; T= 25 °C.

The dramatic decrease of TOC conversion evidenced after 240 minutes of reaction for low oxidant concentration and high catalyst concentration (Figure 3.d) is due to the absence of hydrogen peroxide as promoter of hydroxyl radicals – almost complete conversion of hydrogen peroxide was detected after 75 minutes of reaction. However, a larger amount of hydrogen peroxide with high catalyst loadings (1.5 g/L) leads to an outstanding enhancement of TOC conversion, which is observed even at initial reaction times. Thus, after 240 minutes,

TOC conversions higher than 80 % were attained with 1.5 g/L of catalyst and 4100 ppm of H₂O₂

A possible explanation of these results, as early mentioned, might be the contribution of dark-Fenton reactions under strong oxidant conditions. In order to corroborate this hypothesis two additional catalytic experiments were carried out with high and low concentration levels of both oxidant and catalyst in the absence of UV radiation. Thus, for oxidant and catalyst concentrations of 4100 ppm and 1.5 g/L, without UV radiation, 22% of TOC removal was achieved, whereas hardly 3% of TOC removal was obtained for lowest values of 800 ppm and 0.5 g/L. The decrease of TOC concentration by adsorption of the organic compounds on the catalyst surface has been up to 8% for catalyst loadings of 1.5 g/L. These results clearly reveal a significant contribution of dark-Fenton reactions to the overall catalytic degradation when both high catalyst loadings and strong oxidant conditions are present. Conversely, for very low catalyst loadings (0.5 g/L), TOC removal is not significantly enhanced with hydrogen peroxide concentration. This detrimental effect of high hydrogen peroxide could be explained in terms of reaction (12). An excess of oxidant can favour its reaction with hydroxyl radicals (responsible for the direct oxidation of the organic matter) precluding the extent of mineralization. This negative effect has been also reported for iron-based homogeneous Fenton and photo-Fenton systems [16]:



Figure 4 shows the degradation of aromatic compounds, i. e. phenol, cathecol and hydroquinone (calculated as described in the Experimental Section) and the hydrogen peroxide conversion for the three levels of oxidant concentration at both minimum and

maximum catalyst loadings (0.5 and 1.5 g/L, respectively). Aromatic degradation values above 70% are achieved for both high and low catalyst concentration after 75 minutes of reaction regardless hydrogen peroxide concentration. On the other hand, just a slight increase in aromatic removal is observed as the catalyst concentration increases. Values of aromatic removal close to 100 % are attained after 240 minutes of reaction independent on the oxidant and catalyst concentration.

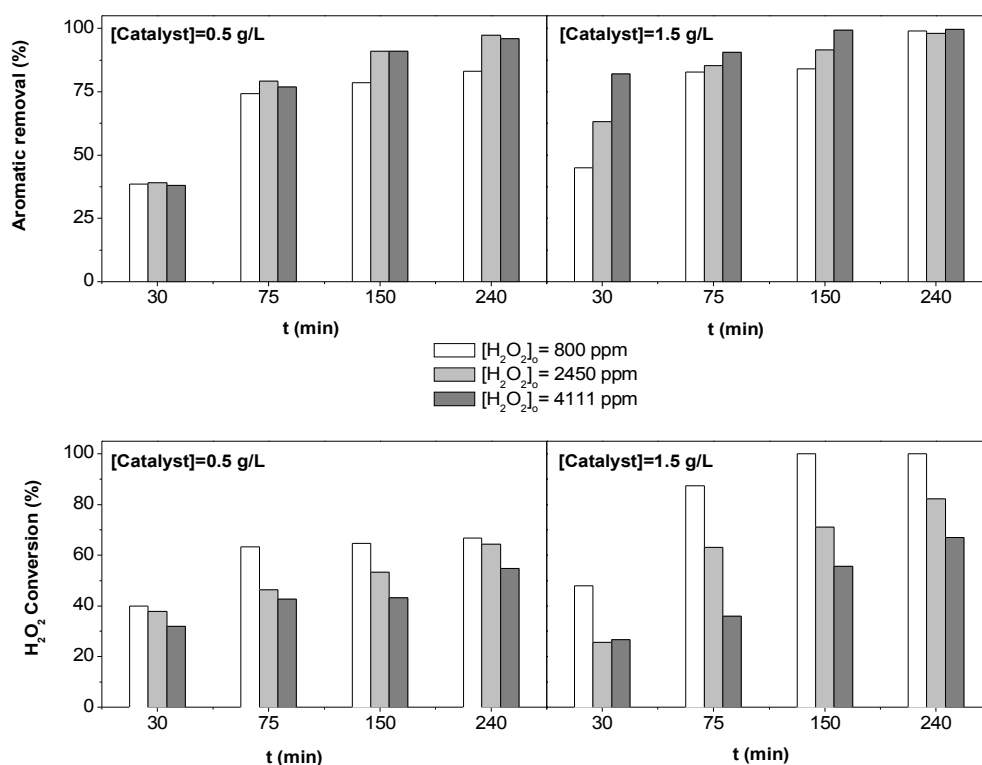


Figure 4. Aromatic removal and oxidant conversion for different initial hydrogen peroxide concentrations at two catalyst loadings. $[TOC]_0=380$ ppm; Initial pH= 5.5; T= 25 °C.

Hydrogen peroxide conversion increases with the reaction time, as expected, being this effect more evident at higher catalyst concentrations. Plots in Figure 4 also show a proportional decrease of H₂O₂ conversion with the increasing of initial concentration of

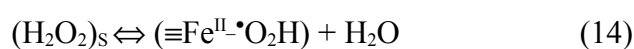
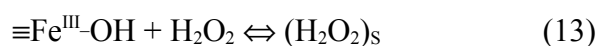
oxidant for each catalyst concentration. It is also observed that for the lowest initial oxidant concentration and the highest catalyst loading, a complete consumption of hydrogen peroxide is produced, conditions at which complete removal of the aromatic material is attained (240 min; 800 ppm of H₂O₂; 1.5 g/L catalyst).

3.4. Induced-photo iron leaching

Leaching experiments studies of iron species from Fe-SBA-15 catalyst during photo-Fenton degradation of phenol were performed in order to ascertain the strength of the iron species supported into SBA-15 mesoporous matrix and the possible contribution of dissolved iron ions in the homogeneous catalytic reactions. Figures 5.a illustrates the iron concentration dissolved into the aqueous solution after 240 minutes of reaction for the set of experiments carried out in our factorial design. Iron concentrations ranging from ca. 2.5 to 11.5 ppm are detected into the aqueous solution depending on the studied reactions conditions. The resistance of iron species to be leached out seems to be related with the oxidant to catalyst ratio. In this sense, several hypothesis can be suggested to figure out the relationship between the experimental conditions and the dissolution of iron species from the catalyst.

In the set of reactions carried out at different hydrogen peroxide loadings for a given catalyst concentration, iron leaching shows a general decreasing trend as oxidant concentration is increased, a trend that is more accentuated for higher catalyst concentrations. This behavior of lower metal leaching for stronger oxidant conditions appears to be different to that shown by heterogeneous catalytic Fenton like-reactions under dark conditions in which the more significant metal leaching phenomenon was observed for high hydrogen peroxide concentrations [27]. In this sense, it has been reported that catalytic decomposition of

hydrogen peroxide over iron oxides is based on the formation of peroxide complex species with Fe(III) active sites on the catalyst surface following of a series of reactions in which this metal surface complex undergoes different electronically excited states until dissociation in peroxide radical [28]. The schematic path of reactions would be the following:



According to this reaction scheme, reduced iron sites can react with hydrogen peroxide to regenerate oxidized iron sites again. From this mechanism, the general decrease of iron leaching for high oxidant concentrations could be attributed to the shielding effect of surrounding metal-H₂O₂ complex species which prevents photo-induced leaching phenomenon by UV-visible irradiation.

Other researches have also proposed the reasonable hypothesis of leaching of Fe^{II} from Fe^{III} containing catalysts as a result of photochemical reduction of Fe^{III} species [29-30] being accumulated in the aqueous phase unless it becomes reoxidized by an excess of hydrogen peroxide. This hypothesis is also in agreement with our results.

Looking at the stability of catalyst in terms of percentage of iron dissolved with respect to the initial content present in the fresh catalyst (Figure 5.b), a significant increase of iron leaching degree is observed for catalyst loadings of 1g/L in comparison with the lower and higher contents for the three levels of oxidant concentration. These results indicate a complex

behavior of the stability of catalyst in photo-Fenton systems, being strongly dependent on the reaction conditions. As it has been mentioned, UV irradiation and the role of hydrogen peroxide in the shielding effect by iron- H_2O_2 complex or in the reoxidation of dissolved Fe(II) ions into the solution can be considered as main arguments to justify the stability of the catalyst.

Therefore, in the case of a catalyst loading of 0.5 g/L, in which a low catalyst to oxidant ratio is present for the three levels of oxidant concentration, the effect of hydrogen peroxide excess seems to be the main reason to explain the lower iron leaching degrees shown in comparison to set of experiments carried out a 1g/L. On the other hand, as irradiation might be another important factor of photo-induced leaching, the scattering UV-visible light phenomenon mediated by greater catalyst concentrations may account for the lower iron leaching degrees observed for 1.5 g/L catalyst loading as compared to that found for 1 g/L. It must be also noteworthy that the influence of pH in the final solution could be another important point for the explanation of the stability of catalyst which will be subject in future studies.

Finally, it must be also noted the progressive increase of iron leaching with reaction time for all the tested reactions, although in different extension depending on the reaction conditions (data for particular reaction conditions are shown in Figure 6). This behavior is very different to that found by Feng et al. [13] with iron laponite RD clays as catalysts in which maximum concentrations of iron ions were detected after 45 minutes of reaction followed by a continuous decrease up to 90 minutes. Although a reasonable explanation has not been reported for these results yet, it can be deduced that the reason of this different

behavior in iron leaching for photo-Fenton systems should be related to the specific nature of the catalyst, probably involving different mechanisms.

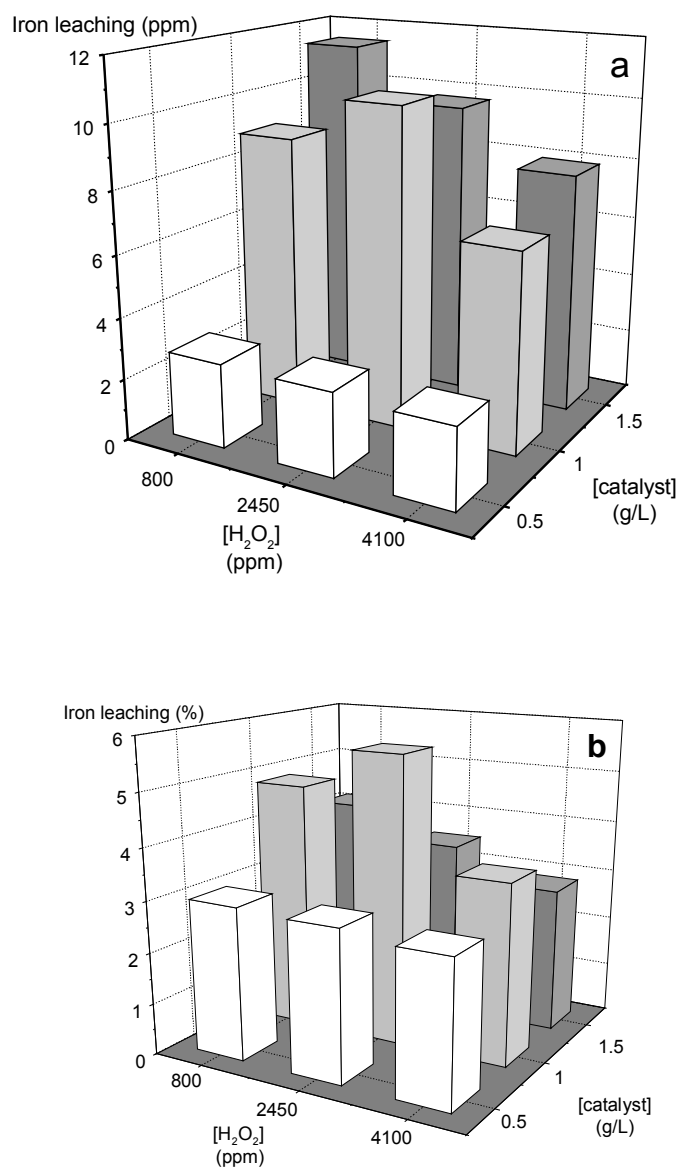


Figure 5. Stability of Fe-SBA-15 catalyst in terms of (a) iron concentration detected into the aqueous solution (b) percentage of iron leached out from the catalysts, after 240 minutes of reaction. [TOC]₀=380 ppm; Initial pH= 5.5; T= 25 °C.

3.4. Influence of homogeneous photo Fenton reactions

In order to ascertain the influence of the iron species leached out into the aqueous solution, additional experiments were carried out using iron (III) chloride as metal source for homogeneous testing reactions. The iron concentration determined in aqueous solution after 240 minutes for the heterogeneous system was found to range from 2.5 to 11.5 ppm (data corresponding to Figure 5.a). In particular, heterogeneous experiments carried out with a hydrogen peroxide concentration of 2450 ppm and catalyst loadings of 0.5 and 1.5 g/L have led to dissolution of iron species up to ca. 2.7 and 9.7 ppm, respectively, after 240 minutes of reaction. With the purpose of comparison, iron concentrations of 3 and 11 ppm were chosen for the homogeneous reaction tests, keeping 2450 ppm as initial hydrogen peroxide concentration. The evolution of TOC and iron concentration in aqueous solution for the homogeneous and heterogeneous runs are shown in Figure 6.

Increasing iron concentration in the homogeneous runs reveals a slight enhancement of TOC removal up to reaction times of 150 minutes. However, a remarkable increase of TOC conversion is observed for the homogeneous run with 11 ppm iron concentration at 240 minutes. Interestingly, the evolution of TOC degradation for homogenous systems is significantly lower than that shown by the heterogeneous ones, especially for the initial reaction times. Moreover, it should be pointed out that the concentration of dissolved iron species coming from the heterogeneous catalyst is much lower for initial reaction times, where much higher TOC removal differences are produced. These results evidence that Fenton homogeneous contribution might occur in parallel with immobilized Fenton process but the remarkable contribution of iron-containing SBA-15 catalyst to the overall

photocatalytic process is also clearly demonstrated, especially at initial reaction times where TOC degradation rate is higher.

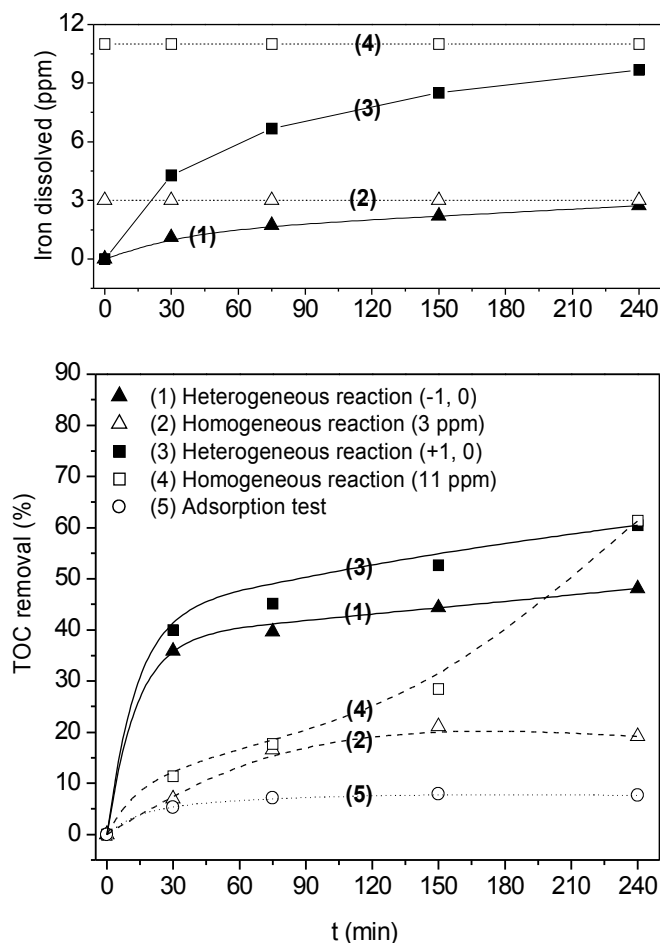


Figure 6. Contribution of homogeneous iron species versus heterogeneous catalytic systems in photo Fenton processes. $[\text{TOC}]_0 = 380$ ppm; $[\text{H}_2\text{O}_2]_0 = 2450$ ppm; Initial pH= 5.5; T= 25 °C.

Finally, an experiment of phenol adsorption was carried out using 1.5 g/L of catalyst concentration in absence of oxidant with the purpose of checking the TOC reduction attributed to the adsorption phenomena. The results shown in Figure 6 clearly indicate the negligible contribution of organic adsorption in the pollutant degradation.

4. Conclusions

Iron-containing SBA-15 catalyst consisting of crystalline hematite particle oxides supported onto a mesostructured silica matrix has been shown as a promising catalyst for the treatment of phenolic solutions through photo-Fenton processes. The outstanding physico-chemical properties make this material more attractive than unsupported commercial hematite iron oxide catalyst, leading to a better overall photocatalytic performance. The experimental design model carried out for different levels of catalyst and hydrogen peroxide concentrations has demonstrated that the increase of catalyst loadings from 0.5 to 1.5 g/L does not promote a significant enhancement of TOC removal except for strong oxidant conditions. The stability of the catalyst towards the leaching of iron species is strongly dependent on the oxidant to catalyst ratio. For the highest catalyst and hydrogen peroxide concentrations (1.5 g/L and 4100 ppm, respectively), the amount of iron species detected into the aqueous solution does not exceed 8 ppm. This low leaching is accompanied with a complete removal of aromatic compounds and a TOC conversion of ca. 80 % after 240 minutes of reaction, which is a remarkable result. Finally, the contribution of homogeneous photo-Fenton reactions from the iron species leached out from the catalyst has been proven to be poorly relevant.

Acknowledgements

The authors thank “Spanish Science and Technology Ministry” for the financial support of this research through the project PPQ-2003-03984.

References

- [1] P. R. Gogate, A. B. Pandit, *Adv. Environ. Res.* 8 (2004) 501-552.
- [2] P. R. Gogate, A. B. Pandit, *Adv. Environ. Res.* 8 (2004) 553-597.
- [3] C. Walling, A. Goosen, *J. Am. Chem. Soc.* 95 (1973) 2987-2991.
- [4] V. Nadtochenko, J. Kiwi, *Inorg. Chem.* 37 (1998) 5233-5238.
- [5] EEC List of Council Directives 76/4647. European Economic Community. Brussels, Belgium (1982).
- [6] J. Fernandez, J. Bandara, A. Lopez, P. Albers, J. Kiwi, *Chem. Commun.* (1998) 1493-1494.
- [7] S. Sabhi, J. Kiwi, *Wat. Res.* 35 (2001) 1994-2002.
- [8] J. Fernandez, J. Bandara, A. Lopez, P. Buffat, J. Kiwi, *Langmuir* 15 (1999) 185-192.
- [9] T. Yuranova, O. Enea, E. Mielczarski, J. Mielczarski, P. Albers, J. Kiwi, *Appl. Catal. B: Environ.* 49 (2004) 39-50.
- [10] S. H. Bossmann, E. Oliveros, S. Göb, M. Kantor, A. Göppert, L. Lei, P. L. Yue, A. M. Braun, *Water Sci. Technol.* 44 (2001) 257-262.
- [11] H. E. Feng, S. Xue-you, L. Le-Cheng, *J. Environ. Sci.* 15 (2003) 351-355.
- [12] J. Feng, X. Hu, P. L. Yue, H. Y. Zhu, G. Q. Lu, *Wat. Res.* 37 (2003) 3776-3784.
- [13] J. Feng, X. Hu, P. L. Yue, *Environ. Sci. Technol.* 38 (2004) 269-275.
- [14] P.L. Yue, J. Y. Feng, X. Hu, *Wat. Sci. Technol.* 49 (2004) 85-90.
- [15] A. Bozzi, T. Yuranova, E. Mielczarski, J. Mielczarski, P.A. Buffat, P. Lais, J. Kiwi, *Appl. Catal. B: Environ.* 42 (2003) 289-303.
- [16] M. Pera-Titus, V. Garcia-Molina, M. A. Banos, J. Gimenez, S. Esplugas, *Appl. Catal. B: Environ.* 123 (2003) 1236-1245.
- [17] F. Martínez, Y. Jhan, G. Stucky, J. L. Sotelo, G. Ovejero, J. A. Melero., *Stud. Surf. Sci. Catal.* 142 (2002) 1109-1116.

- [18] D. Zhao, J. Feng, Q. Huo, N. Melosh, G. H. Fredrickson, B.F. Chmelka, G.D. Stucky, *Science* 279 (1998) 548-552.
- [19] K. S. W. Sing, D. H. Everett, R. A. W. Haul, L. Moscow, R. A. Pierotti, J. Rouquerol, T. Siemieniowska, *Pure Appl. Chem.* 57 (1985) 603-619.
- [20] K. Lazar, G. Calleja, J. A. Melero, F. Martinez, R. Molina. Proceedings of the 14th International Zeolite Conference, Cape Town, South Africa, 2004, p 805-812.
- [21] G. E. P. Box, W. G. Hunter, J. S. Hunter, *Statistics for Experiments, an Introduction to Design, Data Analysis and Model Building*, John Willey and Sons, New York, 1978.
- [22] Z. W. Zheng, L. C. Lei, S. J. Xu, P. L. Cen, *J. Zhejiang Univ Sci.* 5 (2004) 206-211.
- [23] A. Cuzzola, M. Bernini, P. Salvadori, *Appl. Catal. B: Environ.* 52 (2004) 117-122.
- [24] E. Neyens, J. Baeyens, *J. Hazard. Mater.* 98 (2003) 33-50.
- [25] F. Torrades, M. Perez, H. D. Mansilla, J. Peral, *Chemosphere* 53 (2003) 1211-1220.
- [26] F. J. Rivas, F. J. Beltrán, O. Gimeno, P. Alvarez, *J. Hazard. Mater.* 96 (2003) 277-290.
- [27] J. L. Sotelo, G. Ovejero, F. Martinez, J. A. Melero, A. Milieni, *Appl. Catal. B: Environ.* 47 (2004) 281-294.
- [28] S. S. Lin, M. D. Gurol, *Environ. Sci. Technol.* 32 (1998) 1417-1423.
- [29] M. Rios-Enriquez, N. Shahin, C. Duran-de-Bazua, J. Lang, E. Oliveros, S. H. Bossmann, A. M. Braun, *Solar Energy* 77 (2004) 491-501.
- [30] A. Bozzi, T. Yuranova, J. Mielczarski, J. Kiwi, *New. J. Chem.* 28 (2004) 519-526.